

# Various Types of Hydrogen Bonds, Their Temperature Dependence and Water–Polymer Interaction in Hydrated Poly(Acrylic Acid) as Revealed by $^1\text{H}$ Solid-State NMR Spectroscopy

Baohui Li,<sup>‡</sup> Lu Xu,<sup>‡</sup> Qiang Wu,<sup>†</sup> Tiehong Chen,<sup>†</sup> Pingchuan Sun,<sup>\*,†</sup> Qinghua Jin,<sup>‡</sup> Datong Ding,<sup>‡</sup> Xiaoliang Wang,<sup>§</sup> Gi Xue,<sup>\*,§</sup> and An-Chang Shi<sup>‡,||</sup>

Key Laboratory of Functional Polymer Materials, Ministry of Education, College of Chemistry and College of Physics, Nankai University, Tianjin, 300071, P. R. China, Department of Polymer Science and Engineering, The School of Chemistry and Chemical Engineering, State Key Laboratory of Co-ordination Chemistry, Nanjing University, Nanjing 210093, P. R. China, and Department of Physics and Astronomy, McMaster University, Hamilton, Ontario L8S 4M1, Canada

Received February 26, 2007; Revised Manuscript Received June 7, 2007

**ABSTRACT:** Various types of hydrogen bonds, their temperature dependence and water–polymer interaction in hydrated poly(acrylic acid) (PAA) were systematically investigated using  $^1\text{H}$  CRAMPS solid-state NMR techniques in the temperature range from 25 to 110 °C. The  $^1\text{H}$  CRAMPS NMR methods are based on a recently developed continuous phase modulation technique for  $^1\text{H}$ – $^1\text{H}$  homonuclear dipolar decoupling. The  $^1\text{H}$  CRAMPS experiments revealed four types of protons in hydrated PAA which are assigned to protons from the mutually hydrogen-bonded COOH groups (1), from the free COOH groups (2), from the COOH groups bounded with water or from water bounded with COOH groups which are undergoing fast chemical exchange mutually (3), and from main chain groups (4), respectively. Furthermore, we proposed double-quantum filtered and dipolar filtered  $^1\text{H}$  CRAMPS experiments to further assign the protons according to their dipolar coupling strength. In addition, high-resolution spin echo  $^1\text{H}$  CRAMPS experiments were further employed to accurately determine the chemical shift of these protons. These NMR techniques were also used to elucidate the molecular mobility of the different groups. It was found that dehydration in PAA promotes the formation of hydrogen bonds between COOH groups. Variable-temperature  $^1\text{H}$  CRAMPS experiments demonstrated that the dissociation of the hydrogen bonds between COOH groups occurs dramatically at lower temperature in hydrated PAA and slowly over a wide range of temperature in dehydrated PAA. It was also found that the dehydration of water bounded with COOH groups in hydrated PAA occurs significantly at high temperature. The NMR results were compared with previous work using DSC and other techniques. Besides undergoing fast chemical exchange, the adsorbed water was also demonstrated in proximity with the free COOH groups and far from the hydrogen bonds between COOH groups by using two-dimensional  $^1\text{H}$ – $^1\text{H}$  spin-exchange NMR experiments.

## Introduction

Hydrogen bonding is a crucial interaction in determining the final property of a variety of polymers and biopolymers. This interaction has been widely employed in preparing miscible polymer blends, layer-by-layer polymer films, self-assembled block copolymers, and functional polymer materials for adsorption and separation.<sup>1</sup> Hydrogen bonds are particularly important in water-containing polymeric systems since water–polymer interaction has significant effects on the structure and properties of water-containing polymers. Polymer can be swollen by the adsorption of water through the formation of hydrogen bond with water. The formation and structure of hydrogen bonds, and the location of mobile and bound water molecules may induce considerable mechanical and chemical changes to the properties of the polymers.<sup>2</sup> For example, ion conductivity in proton-exchange membranes fuel cell depends critically on the state, content and distribution of water molecules.<sup>3</sup> Meanwhile,

because of the chemical and physical interaction between water and polymers or proteins, the state of water may be changed. The state of water in macromolecules has attracted significant attention in the past decades.<sup>4</sup>

Poly(acrylic acid) (PAA) has been extensively studied and has found wide applications in industry because of its ability to form various kinds of hydrogen bonds via carboxyl acid (COOH) side groups with water and/or other polymers. For example, PAA has been used to prepare miscible polymer blends, super-absorbing gels, layer-by-layer (LBL) polymer films and self-assembled block copolymers.<sup>5</sup> The final properties of the PAA or PAA-containing polymers are intrinsically linked to the quantity, structural environment, and behavior of the carboxyl acid side groups. These groups are classified according to their hydrogen-bond formation and their communication or accessibility to water or other polymers. PAA has received substantial attention, and Fourier-transform infrared (FT-IR) and Raman (FT-Raman) spectroscopy have been widely used to investigate the hydrogen-bonding interaction in PAA and PAA-containing polymers.<sup>6</sup> Dong et al. reported FT-IR and FT-Raman spectroscopy investigations for the coexistence of various hydrogen bond forms in PAA.<sup>6a</sup> Tsukida et al. investigated the effect of neutralization of PAA on the structure of water using Raman spectroscopy.<sup>6b</sup> FT-IR was also used to investigate the phase behavior of the blends of poly(ethylene glycol) with partially neutralization PAA.<sup>6c</sup> Despite these previous works,

\* To whom correspondence should be addressed. Telephone: +86-22-23508171. Fax: +86-22-23494422. E-mail: (P.S.) spclbh@nankai.edu.cn; (G.X.) xuegi@nju.edu.cn.

<sup>†</sup> Key Laboratory of Functional Polymer Materials, Ministry of Education, College of Chemistry, Nankai University.

<sup>‡</sup> College of Physics, Nankai University.

<sup>§</sup> Department of Polymer Science and Engineering, The School of Chemistry and Chemical Engineering, State Key Laboratory of Co-ordination Chemistry, Nanjing University.

<sup>||</sup> Department of Physics and Astronomy, McMaster University.

the determination of different types of hydrogen bonds and, especially, their temperature dependence, as well as the water–polymer interaction in hydrated PAA at a molecular level have not been well understood.

Solid-state NMR (SSNMR) spectroscopy has been proven to be a powerful tool to study the structure and dynamics of polymers and biomacromolecules at a molecular level.<sup>7</sup> Because of its sensitivity to local chemical environments, SSNMR can provide useful information about the microstructure of polymers. Although a variety of SSNMR techniques have been successfully used to study the hydrogen-bonding interactions in polymers and other organic solids,<sup>8</sup> only a small number of NMR studies has been reported to elucidate the structure and temperature dependence of different hydrogen bond form in PAA so far.<sup>9</sup> In a previous work, <sup>13</sup>C CP/MAS and 2D <sup>13</sup>C spin-exchange NMR spectrum have been used to investigate the dynamic alternation between inter- and intra-polymer hydrogen bonds in PAA/poly(ethylene oxide) complex.<sup>10</sup> However, the <sup>13</sup>C SSNMR method requires long experiment time and large amounts of sample because of the poor sensitivity arising from the low abundance of <sup>13</sup>C nuclei. On the contrary, <sup>1</sup>H SSNMR is still the most useful technique due to its high sensitivity to the hydrogen bond strength and the state of water,<sup>3,4b,c,11</sup> although the strong <sup>1</sup>H–<sup>1</sup>H dipole–dipole interaction veils many important structural information. Fast magic angle spinning (MAS)<sup>12</sup> or CRAMPS (combined rotation and multiple-pulse spectroscopy)<sup>13</sup> techniques are commonly used to remove the homogeneous line broadening of protons to obtain well resolved <sup>1</sup>H spectrum. In recent years, SSNMR techniques have achieved significant progress. On the basis of the pioneer work of Emsley's group,<sup>14</sup> the resolution of proton NMR spectrum can be significantly improved using continuous phase modulation technique for <sup>1</sup>H–<sup>1</sup>H homonuclear dipolar decoupling. Continuous phase modulation techniques provide better <sup>1</sup>H–<sup>1</sup>H homonuclear dipolar decoupling at high sample spinning frequencies vs traditional CRAMPS methods.<sup>14c</sup> In combination with dipolar recoupling and multiple-quantum NMR techniques under fast MAS, a variety of high resolution one- and two-dimensional (1D and 2D) <sup>1</sup>H SSNMR experiments have been proposed.<sup>14,15</sup> Detailed information about the structure and dynamics can be directly obtained by <sup>1</sup>H SSNMR spectroscopy. This allows us to directly detect various types of hydrogen bonds, their temperature dependence and water–polymer interaction in solid or semisolid polymers through the direct observation of proton chemical shift related to different chemical groups.

In this study, we focused our attention on systematically elucidating different types of hydrogen bonds and their temperature dependence, as well as water–polymer interaction in hydrated PAA. To achieve these goals, we used a variety of 1D and 2D <sup>1</sup>H CRAMPS solid-state NMR methods based on continuous phase-modulation technique. The <sup>1</sup>H CRAMPS experiments were first used to determine various types of protons. Furthermore, double-quantum filtered and dipolar filtered <sup>1</sup>H CRAMPS experiments were proposed to assign these protons and their associated hydrogen bonds according to the proton–proton dipolar coupling strength. High-resolution spin echo <sup>1</sup>H CRAMPS experiments were then employed to accurately determine the chemical shift of these protons. These techniques were also used to elucidate the molecular mobility of different groups. The variable-temperature (VT) CRAMPS experiments were utilized to determine the temperature dependence of various types of hydrogen bonds. The VT-CRAMPS results were further compared with the results from DSC and other techniques. Finally, 2D <sup>1</sup>H–<sup>1</sup>H spin-exchange NMR

experiments were employed to elucidate the proximity among different protons.

## Experimental Section

**Materials and Preparation of Samples.** Poly(acrylic acid) (PAA) with average molecular weight ( $M_w$ ) of 100000 was purchased from Aldrich Chemical Co. in the form of 35 wt % solution in water. Besides the PAA 35 wt % solution sample (abbreviation, PAA0), two other samples, PAA1 and PAA2, prepared with different treatment conditions from PAA0, were also used. PAA1 was prepared by cast from PAA0 and air-dried for 5 days at room temperature with relative ambient humidity (RH) equal to 80%. PAA1 contains about 7 wt % residual water detected by thermogravimetric analyses (see below). PAA2 was prepared by further drying the PAA1 sample under vacuum at 120 °C for 3 h. Further dehydration process of the PAA1 and water swollen PAA2 samples were carried out in a NMR rotor under fast magic angle spinning as described in the following NMR experimental section.

**Differential Scanning Calorimetry (DSC) Measurements.** DSC experiments were performed on a NETZSCH DSC 204 differential scanning calorimeter in dry nitrogen atmosphere. Samples of about 8 mg were placed in the DSC pan with a cap having a vent hole for loss of water. All samples were first heated from 0 to 160 °C at a rate of 20 °C/min (first heating scan) and kept at that temperature for 2 min; subsequently, they were cooled to 0 °C at a rate of –20 °C/min and kept at that temperature for 2 min. Following the cooling scan, a second heating scan was conducted with the same heating rate as the first one. The midpoint of the slope change of the heat capacity plot was taken as the glass transition temperature ( $T_g$ ).

**Thermogravimetric Analyses (TGA).** TGA experiments were performed on a NETZSCH TG 209 instrument at a linear heating rate of 20 °C/min from 0 to 300 °C under nitrogen atmosphere.

**NMR Experiments.** Liquid-state <sup>1</sup>H NMR experiments were performed on a Varian UNITYplus-400 narrow-bore (54 mm) NMR spectrometer operating at a proton frequency of 400.1 MHz. 3 mg of PAA2 was dissolved in 0.5 mL 99.9% deuterated water (D<sub>2</sub>O, Cambridge Isotope Laboratories, Inc.), PAA0 was directly put into the NMR tube without using D<sub>2</sub>O and <sup>1</sup>H chemical shift was referenced to external TMS. Solid-state NMR experiments were performed on a Varian Infinityplus-400 wide-bore (89 mm) NMR spectrometer operating at a proton frequency of 399.7 MHz. A conventional 4 mm double-resonance HX CP/MAS NMR probe was used for all CRAMPS experiments, and samples were placed in a 4 mm zirconia PENCIL rotor with 52  $\mu$ L sample volume. The magic angle spinning (MAS) was automatically controlled at 9.8 kHz within  $\pm 2$  Hz with a MAS speed controller for all 1D and 2D experiments. This special spinning frequency was chosen to avoid the recoupling of anisotropic interaction when using DUMBO-1 decoupling under MAS condition as reported in previous work<sup>14b</sup> and to provide better resolution. Variable-temperature <sup>1</sup>H CRAMPS NMR experiments were carried out in the temperature range of 25–110 °C with a Varian Model-L950 temperature controller, a temperature equilibration period of 4 min was used before NMR spectra were acquired at each measurement temperature. The recycle delay was set to 3 s. Several 1D and 2D <sup>1</sup>H SSNMR pulse sequences based on continuous phase modulation technique for <sup>1</sup>H–<sup>1</sup>H homonuclear dipolar decoupling, DUMBO-1 and eDUMBO-1 proposed by Emsley et al.,<sup>14</sup> were used in this study. The DUMBO-1 and eDUMBO-1 decoupling cycle time was set to 32  $\mu$ s divided in 64 discrete phase steps of 500 ns duration each, and <sup>1</sup>H decoupling RF field strength of DUMBO-1 and eDUMBO-1 were set to 100 kHz in both dimensions. The <sup>1</sup>H chemical shift was calculated using an experimentally determined scaling factor of 0.58 and was externally referenced using the continuous phase modulated <sup>1</sup>H CRAMPS spectrum of alanine relative to tetramethylsilane (TMS) (CH<sub>3</sub>)<sub>4</sub>Si ( $\delta$  = 0 ppm). Figure 1 shows the pulse sequences for various <sup>1</sup>H SSNMR experiments used in this work, and they will be explained individually in the following corresponding experiments. The verification of <sup>1</sup>H

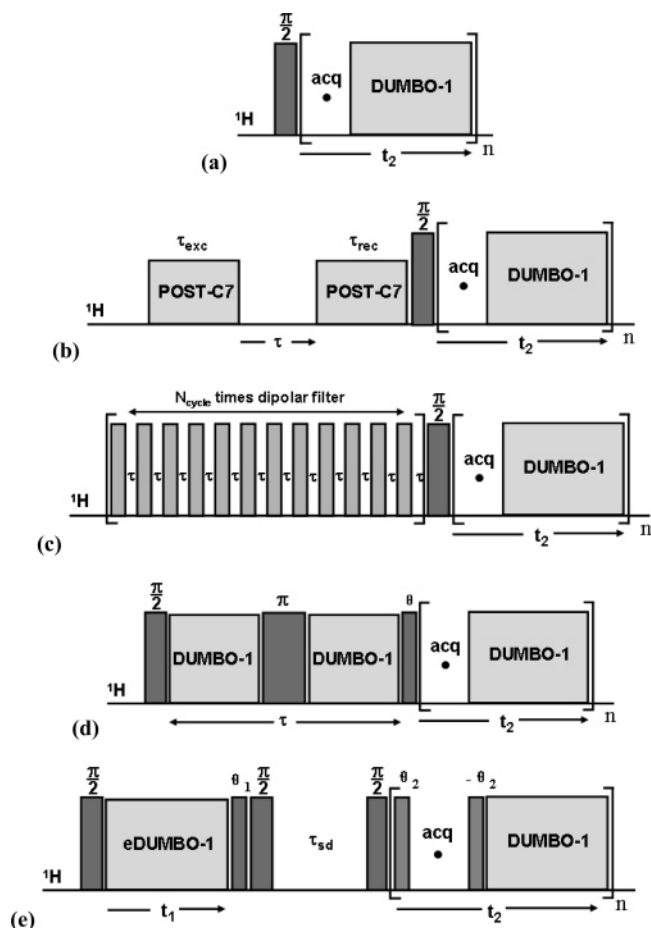


**Figure 1.** Pulse sequences for various  $^1\text{H}$  CRAMPS NMR experiments recorded with DUMBO-1 homonuclear decoupling during  $t_2$ : (a)  $^1\text{H}$  PM-CRAMPS experiment; (b)  $^1\text{H}$  DQ-CRAMPS experiment; (c)  $^1\text{H}$  DF-CRAMPS experiment; (d)  $^1\text{H}$  SE-CRAMPS experiment; (e) 2D  $^1\text{H}$ – $^1\text{H}$  spin-exchange CRAMPS experiment.

SSNMR experimental conditions for DUMBO-1 based  $^1\text{H}$  CRAMPS experiments and calibration of the scaling factor using alanine powder sample as a reference were described in the Supporting Information.

**(1)  $^1\text{H}$  CRAMPS Experiment Based on Continuous Phase Modulation Technique (PM-CRAMPS).**<sup>14a</sup> This experiment is used to obtain high-resolution  $^1\text{H}$  NMR spectrum of organic solids. Figure 1a shows the pulse sequence; the detection windows with 5  $\mu\text{s}$  delay were inserted between two DUMBO-1 decoupling cycles, yielding a dwell time of 37  $\mu\text{s}$ . The  $90^\circ$  pulse length was 2.5  $\mu\text{s}$ . To avoid the spectral broadening effect under fast MAS condition, the rotor period was carefully adjusted so that it is not an integral multiple of the cycle time of the DUMBO-1 cycle.<sup>14a</sup> Same parameters were used in the following experiments.

**(2) Double-Quantum (DQ) Filtered and Dipolar Filtered (DF)  $^1\text{H}$  CRAMPS Experiments (DQ-CRAMPS and DF-CRAMPS):** A variety of techniques have been developed to select magnetization with strong or weak dipolar coupling in solids. On the basis of previous work of DQ filter<sup>15b</sup> and DF filter<sup>17</sup> NMR methods, we proposed two new 1D  $^1\text{H}$  CRAMPS NMR experiments, namely DQ-CRAMPS and DF-CRAMPS, to distinguish the different types of protons in PAA according to their  $^1\text{H}$ – $^1\text{H}$  dipolar coupling strength associated with their difference in molecular mobility.

Figure 1b shows the  $^1\text{H}$  DQ-CRAMPS pulse sequence to select magnetization of rigid protons, which is based on the 2D DQ MAS NMR experiment proposed by Emsley et al. recently.<sup>16a</sup> Double-quantum excitation and reconversion is achieved by using the POST-C7 pulse sequence.<sup>15a</sup> POST-C7 is a DQ dipolar recoupling pulse sequence with a phase dependence on the rotor phase. The DQ excitation ( $\tau_{\text{exc}}$ ) and reconversion ( $\tau_{\text{rec}}$ ) time were set to 58.3

$\mu\text{s}$  at 9.8 kHz MAS, and the DQ evolution time  $\tau$  was fixed to 1  $\mu\text{s}$ . The detection period is the same as that used in  $^1\text{H}$  PM-CRAMPS experiment. By an appropriate selection of the excitation/reconversion periods of the double-quantum coherences, the magnetization of the protons with strong dipolar couplings would pass through the filter, whereas that of the weaker dipolar couplings will be filtered out. A similar  $^1\text{H}$  DQ-filter spin diffusion NMR experiment, using BABA dipolar recoupling pulse sequences under fast MAS, was also reported to determine the domain size of polymer membranes.<sup>16b</sup> In addition, Lesage et al. also proposed a novel 2D DQ-filtered  $^1\text{H}$ – $^{13}\text{C}$  HETCOR NMR technique using  $^{13}\text{C}$  detection instead of  $^1\text{H}$  detection.<sup>16c</sup>

Figure 1c shows the  $^1\text{H}$  DF-CRAMPS pulse sequence to select the magnetization of mobile protons. Several cycles ( $N_{\text{cycle}}$ ) of 12-pulse dipolar filter are used to select the  $^1\text{H}$  magnetization from the mobile protons which have longer transverse relaxation times than those of rigid protons.<sup>17</sup>  $^1\text{H}$  PM-CRAMPS is then used to detect the  $^1\text{H}$  signals. The  $90^\circ$  pulse length in dipolar filter is 2.5  $\mu\text{s}$  and the inter-pulse spacing of  $\tau$  is typically 8–12  $\mu\text{s}$ .

**(3) Spin-Echo  $^1\text{H}$  CRAMPS Experiments (SE-CRAMPS):** This experiment was proposed by Emsley et al.<sup>14b</sup> and used for measuring proton transverse dephasing times under DUMBO-1 dipolar decoupling. In this work, we use this experiment to obtain high-resolution  $^1\text{H}$  CRAMPS spectrum, because this experiment provides better resolution than that obtained by PM-CRAMPS and suppresses the signal which have shorter proton transverse dephasing time ( $\tau$ ) under DUMBO-1 decoupling. The pulse sequence of this experiment contains a spin echo pulse in the middle of the two windowless DUMBO-1 dipolar decoupling sequences as shown in Figure 1d. The  $\theta$  pulse compensates for different tilt angles of the effective fields between windowless and windowed DUMBO-1 decoupling.<sup>14b</sup> The dephasing time  $\tau$  was set to 4 ms.

**(4) 2D  $^1\text{H}$ – $^1\text{H}$  Spin-Exchange CRAMPS Experiments.** This experiment is used to study chemical exchange and/or spin diffusion among protons. The pulse sequence of this experiment is shown in Figure 1e, which is similar to the 2D  $^1\text{H}$ – $^1\text{H}$  CRAMPS experiments proposed by Caravatti et al.<sup>18</sup> and improved by Emsley et al.<sup>14b,14c</sup> using continuous phase modulation techniques in both the indirect and direct detection to achieve high-resolution 2D  $^1\text{H}$  spectrum. After the first  $90^\circ$  pulse, windowless eDUMBO-1 decoupling<sup>14b</sup> during evolution time  $t_1$  is immediately placed in order to obtain high-resolution  $^1\text{H}$  spectrum in the indirect detection period, the following short  $\theta_1$  pulse corresponding to  $54.7^\circ$  is applied which rotates the proton magnetization from the tilted transverse plane to the ( $x$ ,  $y$ ) plane of the rotating frame, and then another followed  $90^\circ$  pulse rotates the magnetization to the  $z$  direction. In the following “mixing” period ( $\tau_{\text{sd}}$ ), spin-exchange occurs due to chemical exchange or spin-diffusion. Finally,  $^1\text{H}$  PM-CRAMPS detection is used in the direct detection period ( $t_2$ ) with a short pulse  $\theta_2$  (0.5  $\mu\text{s}$ ) to suppress the quadrature images in  $F_2$ . A TPPI scheme on the second  $90^\circ$  pulse is used for quadrature detection in  $F_1$ .<sup>14b</sup> A total of 200  $t_1$  with 32 scans each was collected. All 2D NMR experiments were performed at room temperature (25  $^\circ\text{C}$ ).

In situ observation of the dehydration process for PAA1 or water swollen PAA2 in our NMR experiments was carried out under rapid sample rotation in the 4 mm CP/MAS probe by means of the flow of drive, bearing and VT gas. The zirconia PENCIL rotor comprises a drive tip, a sample spacer, and a Teflon end-cap. The end-cap has a vent hole to relieve pressure in the rotor and provide an escape route for loss of water from the rotor during the VT experiment. This novel in situ dehydration experiment in a solid-state MAS NMR probe was reported in previous works on sodium acetate and polymer electrolyte membranes, which opens up an alternative pathway for dehydration of samples.<sup>19</sup> On the basis of previous reports on MAS-induced heating in SSNMR,<sup>20</sup> it should be mentioned that the real temperature for samples in our in situ dehydration at 9.8 kHz spinning frequency should be about 5 to 10  $^\circ\text{C}$  higher than the set temperature. It should be also mentioned here that although a better resolution of the  $^1\text{H}$  CRAMPS spectra can be achieved from the projection of a 2D strategy using eDUMBO-1 and DUMBO-1 dipolar decoupling in  $t_1$  and  $t_2$



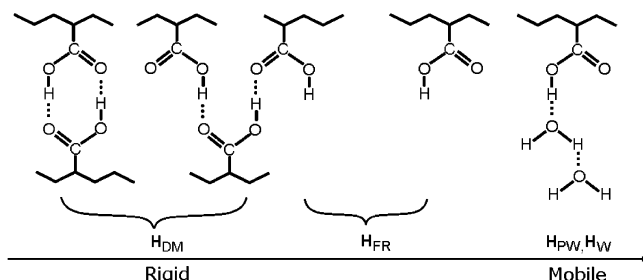


**Figure 2.** Schematic illustration of different types of protons and their associated hydrogen bonds (dot line) in hydrated PAA.

dimensions, we found that the above 1D  $^1\text{H}$  CRAMPS experiments (Figure 1a–d) can provide good resolution in a shorter experimental time, this is very important to perform the in situ VT-CRAMPS NMR experiment at a fixed heating rate. Furthermore, single-pulse fast MAS experiments were performed on a conventional 2.5 mm double-resonance HX CP/MAS NMR probe with a 2.5 mm zirconia PENCIL rotor for comparison in the spectral resolution with CRAMPS experiments.

## Results and Discussion

### 1. Different Types of Protons and Hydrogen Bond Forms, and the Water–Polymer Interaction in Hydrated PAA Determined by $^1\text{H}$ PM-CRAMPS Experiments.

The hydrogen bonds between carboxylic groups of organic acids have long been investigated, and it is well-known that cyclic dimer mainly exist in the pure liquid and solid states.<sup>21</sup> Different hydrogen bonds between the COOH groups in PAA are also suggested in the previous work.<sup>6a,6b</sup> Furthermore, it is generally accepted that three different states of water are present in polymers, known as “bound”, “intermediate”, and “free” water, respectively. On the basis of these previous works, we anticipate that there are different types of protons and they may be associated or not associated with hydrogen bonds in the hydrated PAA samples. For convenience of discussion, we denote these different types of protons with the following abbreviations:  $\text{H}_{\text{DM}}$  represents the protons of hydrogen bonds between COOH groups including cyclic and open COOH dimers as described in ref 6a,  $\text{H}_{\text{FR}}$  represents the non-hydrogen-bonded protons on isolated COOH or open COOH dimer,  $\text{H}_{\text{PW}}$  represents the COOH protons which can form hydrogen bonds with water, and  $\text{H}_{\text{W}}$  represents the water protons which can form hydrogen bonds with polymer (bound water) or with other water molecules (intermediate water). These protons are schematically illustrated in Figure 2 (note: protons in the main chain are not shown in the figure). From Figure 2, there exist three types of hydrogen bonds which are associated with  $\text{H}_{\text{DM}}$ ,  $\text{H}_{\text{PW}}$  and  $\text{H}_{\text{W}}$  protons, respectively. The different chemical environment of the protons shown in Figure 2 may significantly affect their  $^1\text{H}$  chemical shift. On the other hand, it is expected that the protons in different chemical environments should exhibit difference in the molecular mobility. In this section, we will use  $^1\text{H}$  PM-CRAMPS experiments to detect various types of protons based on their difference in chemical shift. As the hydrogen bonds are associated with different protons, therefore, the different types of hydrogen bonds can be determined accordingly.

Before carrying out the  $^1\text{H}$  SSNMR experiments, liquid-state NMR experiments were performed to determine the chemical shift of different protons and possible chemical exchange between water and COOH groups in PAA solutions. Figure S2a in the Supporting Information shows the liquid-state  $^1\text{H}$  NMR spectrum of 3 mg PAA2 dissolved in 0.5 mL deuterated water. The strong peak at 4.8 ppm should be assigned to free water, while the peak at 2.5 ppm and the peaks around 1.8 ppm should

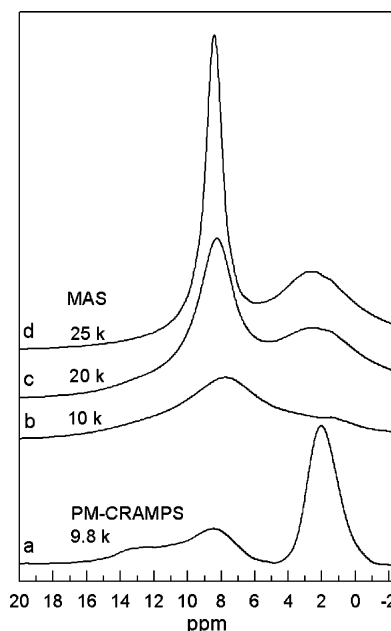


**Figure 3.**  $^1\text{H}$  solid-state NMR spectra of PAA1: (a) PM-CRAMPS spectrum at 9.8 kHz spinning frequency, and single-pulse  $^1\text{H}$  MAS spectra at spinning frequencies of (b) 10, (c) 20, and (d) 25 kHz, respectively.

be assigned to the methine and methylene protons of PAA, respectively. Figure S2b in the Supporting Information shows the liquid-state  $^1\text{H}$  NMR spectrum of PAA0. Besides the main chain protons, only one strong peak at 5.2 ppm associated with water was found. Since the peak of COOH group is absent and the water peak shifts to the low field, therefore, we can conclude that the protons of COOH groups ( $\text{H}_{\text{PW}}$ ) should undergo fast chemical exchange with water protons ( $\text{H}_{\text{W}}$ ) in PAA 35 wt % solution, as denoted in Figure S2b by arrows between  $\text{H}_{\text{PW}}$  and  $\text{H}_{\text{W}}$ . For convenience of the following discussion, we will still assign this peak for water although which is actually the averaged signal resulting from the chemical exchange between water and COOH groups.

Before we performed the CRAMPS NMR experiment in this study, we first compared the spectral resolution of PAA1 using fast MAS technique with that obtained by DUMBO-1 based CRAMPS technique, and the results are shown in Figure 3. It is noteworthy that the spectral resolution of the PAA1 obtained by PM-CRAMPS at 9.8 kHz is obviously much higher than those obtained by MAS even at fast spinning frequency of 25 kHz, whereas the spectrum obtained by MAS at 9.8 kHz is almost featureless. This demonstrates that DUMBO-1 based CRAMPS, instead of fast MAS, is a better technique in line-narrowing for hydrated PAA sample and was employed in the following study. In principle,  $^1\text{H}$  CRAMPS experiment can provide quantitative information if there are no other influence besides the dipolar coupling. However, there are offset/chemical-shift-depending scaling factors and decoupling efficiency depends on the offset, also interferences with MAS and molecular motion.<sup>22</sup> Therefore, CRAMPS is usually qualitative in practice. Without special notation, the spectral intensities of CRAMPS peaks in the following discussion are interpreted in a relative sense within the same spectrum.

The solid-state  $^1\text{H}$  PM-CRAMPS NMR spectra of PAA0 at different dehydration time from 1 day to 5 days (i.e., PAA1) at room temperature with a relative humidity (RH) of 80% are shown in Figure 4. Figure 4a shows that one strong peak at 7.1 ppm and one weak and broaden peak at 2.0 ppm can be clearly observed for the 1-day dried sample. Compared with Figure

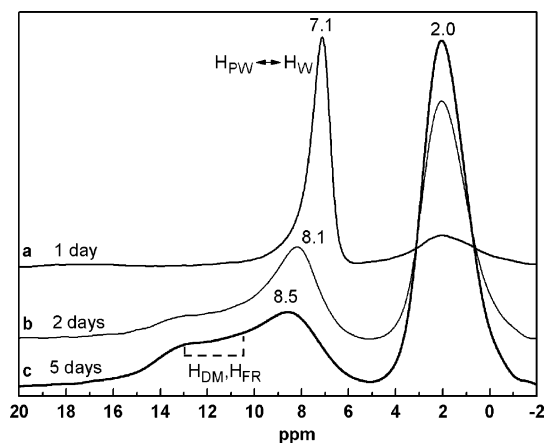


**Figure 4.**  $^1\text{H}$  PM-CRAMPS NMR spectra of PAA0 at dehydration time of (a) 1 day, (b) 2 days, and (c) 5 days (PAA1).

S2b, the peak at 2.0 ppm should be assigned to the overlapped signals of the methine and methylene protons of PAA, and the strong peak at 7.1 ppm should be reasonably assigned to the protons of large cluster of water molecules ( $\text{H}_\text{W}$ ) that are mutually hydrogen bonded and/or also interact with the COOH side groups, as well as the COOH groups undergoing fast chemical exchange with water ( $\text{H}_\text{PW}$ ). It is observed that the signal of water at 7.1 ppm gradually broadens and shifts to 8.5 ppm with increasing the dehydration time from 1 to 5 days, which indicates that the chemical shift of water signal depends strongly on the water content. This is also a clear evidence of the chemical exchange between water and PAA COOH groups. The decreasing and broadening of the water peak shown in Figure 4 also suggest that the amount of the intermediate water decreases while that of the bound water increases with increasing the dehydration time. A similar behavior of the water signal adsorbed in PVDF-g-PSSA polymer electrolyte membrane was also observed by Hietala et al.<sup>3b</sup>

It is well known that molecular motion can destructively interfere with line-narrowing by CRAMPS.<sup>22</sup> If the center of the correlation time distribution describing molecular motion (or proton exchange) comes close to the cycle time of the DUMBO-1 multiple pulse sequence, the effectiveness of the DUMBO-1 decoupling will be reduced. It is noted that the peak of PAA main chain protons at 2.0 ppm in Figure 4a is remarkably broad. Because this sample contains large amount of residual water and the sample is quite mobile after 1 day's dehydration from PAA0, therefore, we suggest that the broadening of this peak could be attributed to the motional interference with DUMBO-1 decoupling. The relative intensity of this peak increases and its line width narrows remarkably after dehydration of PAA0 from 2 to 5 days as shown in Figure 4, parts b and c. This can be attributed to the dehydration and decrease of the molecular mobility of PAA during dehydration, which results in a considerable increase of the dipolar interaction among the PAA main chain protons and reduction of the interference between molecular motion with CRAMPS, thus enhances the efficiency of DUMBO-1 dipolar decoupling.

It is noteworthy that a new broad peak at about 10–13 ppm occurs after 2 days dehydration and increases with further dehydration, while the chemical shift of this broad peak keeps unchanged during further hydration. Since dehydration cannot result in the increase of  $\text{H}_\text{PW}$  signals, therefore, the new broad peak at 10–13 ppm should be reasonably assigned to the  $\text{H}_\text{DM}$  and  $\text{H}_\text{FR}$  instead of the  $\text{H}_\text{PW}$  protons. Since  $\text{H}_\text{DM}$  and  $\text{H}_\text{FR}$  signals are seriously overlapped, the accurate assignment of these protons using  $^1\text{H}$  DQ-, DF-, and SE-CRAMPS techniques will

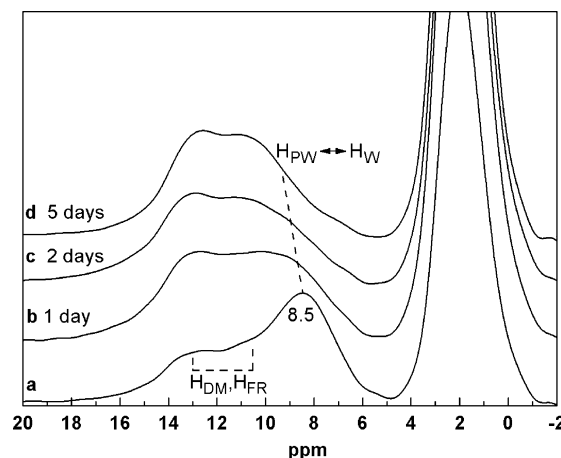


**Figure 5.**  $^1\text{H}$  PM-CRAMPS NMR spectra of (a) PAA1 and that in situ dehydrated at different time in a NMR probe under rapid sample rotation: (b) 1 day, (c) 2 days, and (d) 5 days.

be given in the next section. The above result suggests that the stable hydrogen bonds between COOH groups related to  $\text{H}_\text{DM}$  can easily form in dehydrated PAA and are unfavorable in highly hydrated PAA, and this was further supported by the following experiments (Figure 5).

To investigate the water–polymer interaction and determine the possible range of the chemical shift of water protons undergoing chemical exchange, the dehydration process was further carried out under the condition of rapid sample rotation in the solid-state MAS probe.<sup>19</sup> Figure 5 shows the  $^1\text{H}$  PM-CRAMPS spectra of PAA1 under continuous flowing dry air in a NMR probe at different dehydration time. These spectra were obtained under the same experimental condition and displayed in the same scale. During the dehydration process, the water signal at 8.5 ppm continuously broadens, decreases in intensity due to the dehydration during MAS and shifts to the low field near 9 ppm. On the other hand, the broad peak at 10–13 ppm associated with  $\text{H}_\text{DM}$  and  $\text{H}_\text{FR}$  obviously increases with the dehydration. Our experiment demonstrates that rapid sample rotation in a solid-state NMR probe is an alternative pathway for dehydration of the sample. As reported in previous work,<sup>19a</sup> the rate of dehydration was also found to depend on the rotation frequency. Hong et al.<sup>19c</sup> reported that spinning of the hydrated membrane samples at ambient temperature for an extended period of time was prone to cause dehydration. Since no obvious change of the spectrum can be found under further dehydration in the NMR probe, our NMR experiments indicate that the final equilibrium dehydration of the PAA1 sample can be achieved at about 5 days at room temperature.

To monitor the chemical shift change of water during hydration and dehydration, and to avoid the effect of strong water signal on the observation of other peaks, we used deuterated instead of hydrogenated water to investigate the hydration process of the vacuum-dried sample PAA2. Figure 6 shows the  $^1\text{H}$  PM-CRAMPS spectra of PAA2 and of the sample prepared by adding a small drop of deuterated water in PAA2 then dehydrated in a NMR probe at different time. In Figure 6a, we can observe two overlapped peaks at range of 10–13 ppm for PAA2. Since PAA2 contains little residual water, therefore, we can reasonably assign these two peaks to the overlapped  $\text{H}_\text{DM}$  and  $\text{H}_\text{FR}$  protons. After adding a small drop of deuterated water (Figure 6b), we can clearly observe that water signal at around 7.6 ppm occurs and it gradually broadens and shifts to the low field at about 9 ppm with dehydration. By comparing the spectra of PAA2 dehydrated under vacuum

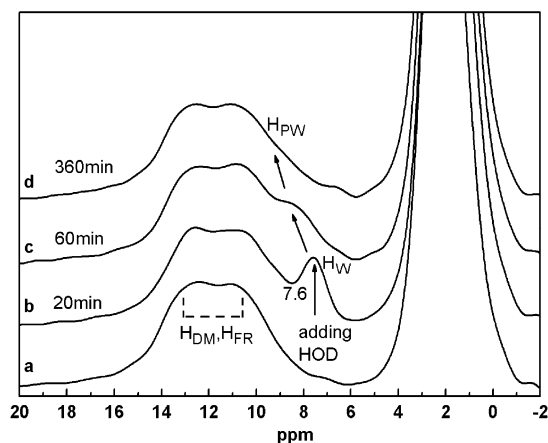


**Figure 6.**  $^1\text{H}$  PM-CRAMPS NMR spectra of (a) PAA2 and of the sample prepared by adding a small drop of deuterated water in the PAA2 sample then in situ dehydrated at different time in a NMR probe under rapid sample rotation: (b) 20 min, (c) 60 min, and (d) 360 min.

condition (Figure 6a) with that of the samples dehydrated under rapid sample rotation in the NMR MAS probe (Figure 5d or 6d), it is noticed that a complete dehydration of PAA cannot be achieved in the NMR probe at room temperature.

**2. Assignment of Different Types of Protons and Hydrogen Bonds by Double-Quantum and Dipolar Filter, as Well as Spin Echo  $^1\text{H}$  CRAMPS Experiments.**  $^1\text{H}$  double-quantum and dipolar filter MAS NMR techniques have been widely used to determine the  $^1\text{H}$ – $^1\text{H}$  dipolar coupling and heterogeneous dynamics in organic solids in the past decade.<sup>15–17</sup> Since both the excitation and subsequent reconversion of DQ coherence relies on the presence of a dipolar coupling between a particular pair of spins close together in space,  $^1\text{H}$  DQ MAS experiment can be used to identify proton–proton proximities within 0.35 nm and distinguish protons with different molecular mobility. Recently, Lesage et al. reported an investigation of dipolar-mediated water–protein interactions in microcrystalline protein by using novel 2D DQ-filtered  $^1\text{H}$ – $^{13}\text{C}$  HETCOR NMR techniques.<sup>16c,25a</sup> From the above  $^1\text{H}$  PM-CRAMPS experiments, we have observed different types of protons in hydrated PAA, however, the peaks at range of 10–13 ppm are seriously overlapped. To further assign these protons and reveal various hydrogen bond forms, we employed  $^1\text{H}$  DQ- and DF-CRAMPS experiments to distinguish these protons according to their  $^1\text{H}$ – $^1\text{H}$  dipolar coupling strength which is related to their molecular mobility. In principle, various NMR methods can be used to select protons with different dipolar coupling or molecular mobility, such as DF and DQ filter. The DF filter method<sup>17</sup> is convenient to select protons with weak dipolar coupling; in contrast, DQ filter<sup>15,16</sup> is suitable to select protons with strong dipolar coupling. Both of them are used here since there are both weak and strong dipolar couplings in the PAA samples. In addition, we also employed high-resolution spin echo  $^1\text{H}$  CRAMPS experiments to accurately determine the chemical shift of different protons, because this experiment provides better resolution than that obtained by  $^1\text{H}$  PM-CRAMPS experiments.<sup>14b</sup>

Parts a and b of Figure 7 show the  $^1\text{H}$  PM- and DQ-CRAMPS spectra of PAA0 after 1-day dehydration at room temperature, respectively. It is observed that the strong water signal at 7.1 ppm in Figure 7a decreases dramatically in Figure 7b after the DQ-filter, which indicates that the adsorbed water and COOH groups interacting with water are considerably mobile. It is also noticed that the relative intensity of the peak at 2.0 ppm (PAA main chain) increases remarkably after the DQ-filter, which implies that the aliphatic protons are consider-

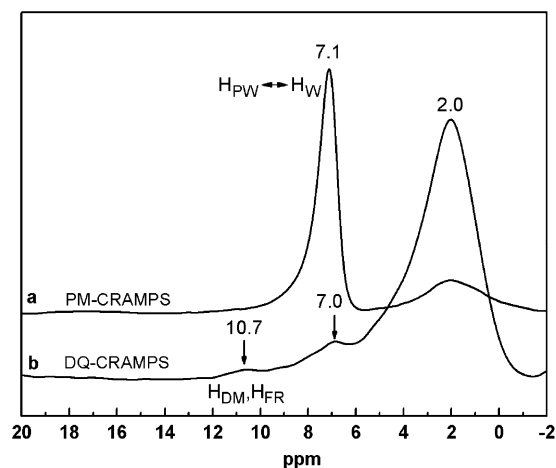


**Figure 7.**  $^1\text{H}$  (a) PM- and (b) DQ-CRAMPS NMR spectra of PAA0 after 1-day dehydration at room-temperature recorded using the pulse sequences as shown in Figure 1, parts a and b, respectively.

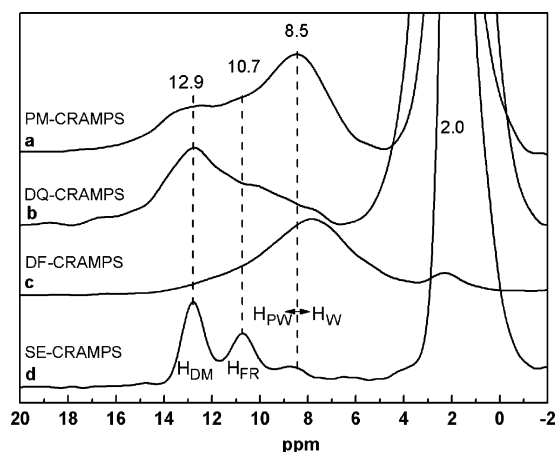


**Figure 8.**  $^1\text{H}$  (a) PM-, (b) DQ-, (c) DF-, and (d) SE-CRAMPS NMR spectra of PAA1 recorded using the pulse sequences shown in Figure 1, parts a–d, respectively.

ably rigid and exhibit strong dipolar coupling. Meanwhile, it is noteworthy that a new weak peak at 10.7 ppm can be observed in the DQ-CRAMPS spectrum (Figure 7b), indicating the protons of this peak have stronger dipolar coupling than that of the water protons. Since  $\text{H}_{\text{PW}}$  and  $\text{H}_{\text{W}}$  undergo fast chemical exchange at room temperature (see Figure 3b) and they cannot be distinguished, therefore, the new peak at 10.7 ppm should be reasonable assigned to  $\text{H}_{\text{DM}}$  and/or  $\text{H}_{\text{FR}}$  protons. The assignment of this peak will be further discussed in the following section. The above results also indicate that DQ-CRAMPS method can efficiently suppress the signals of the mobile groups and provide useful dynamics information on the polymers.

Parts a–d of Figure 8 show the  $^1\text{H}$  PM-, DQ-, DF-, and SE-CRAMPS spectra of PAA1 containing about 7 wt % residual water. The relative intensity of the water signal at 8.5 ppm in Figure 8a decreases dramatically after the DQ-filter in Figure 8b, which indicates that the adsorbed water and COOH groups interacting with water are still considerably mobile in PAA1. Except for the aliphatic protons, it is noteworthy that the relative intensity of the peak at 12.9 ppm in Figure 8a increases remarkably after DQ-filter in Figure 8b, indicating strong dipolar coupling among these protons. Since only  $\text{H}_{\text{DM}}$  protons may have the strongest dipolar coupling than that of other COOH or water protons, therefore, we can reasonably assign the peak at 12.9 ppm to  $\text{H}_{\text{DM}}$  protons. Figure 8c shows the  $^1\text{H}$  DF-CRAMPS spectrum, which selects only the mobile protons with



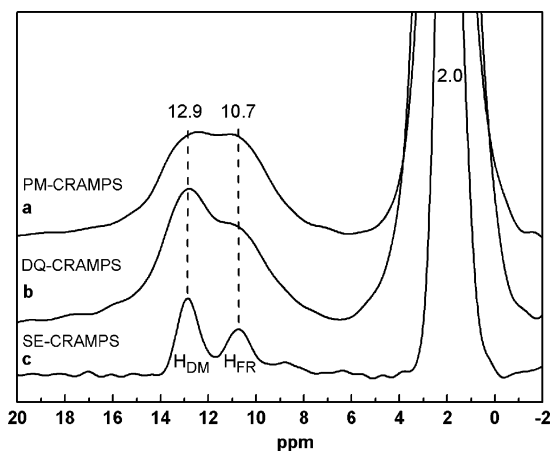


**Figure 9.**  $^1\text{H}$  (a) PM-, (b) DQ-, and (c) SE-CRAMPS spectra of PAA2 recorded using the pulse sequences shown in Figure 1, parts a, b, and d, respectively.

weak dipolar coupling. We noticed that only one broad peak at about 7.8 ppm was observed besides the small peak of aliphatic protons at 2.0 ppm. Because only  $\text{H}_\text{W}$  and  $\text{H}_{\text{PW}}$  protons exhibit high mobility as determined by the above  $^1\text{H}$  DQ-CRAMPS experiments, therefore, the broad peak at about 7.8 ppm can be reasonably assigned to  $\text{H}_\text{W}$  and  $\text{H}_{\text{PW}}$ . These two experiments clearly indicate that  $^1\text{H}$  DQ- and DF-CRAMPS methods are effective NMR techniques to distinguish different types of protons based on their dipolar coupling strength, especially the hydrogen bonded one. Figure 8d shows the  $^1\text{H}$  SE-CRAMPS spectrum with proton transverse dephasing time  $\tau = 4$  ms. This technique can provide higher resolution spectrum than any other  $^1\text{H}$  CRAMPS methods due to the elimination of the signals with short  $T_2$  during the dephasing time, although the sensitivity is lower. It is noteworthy that the line widths of each peak are dramatically narrowed as shown in Figure 8d, and four peaks at 12.9, 10.7, 8.5, and 2.0 ppm can be clearly distinguished. As analyzed earlier, these four peaks can be assigned to  $\text{H}_{\text{DM}}$ ,  $\text{H}_{\text{FR}}$ ,  $\text{H}_{\text{PW}}/\text{H}_\text{W}$ , and aliphatic protons, respectively. It should be emphasized that  $^1\text{H}$  SE-CRAMPS experiment provides accurate chemical shift of different protons and unambiguously confirms the assignment of different types of protons from other  $^1\text{H}$  CRAMPS techniques.

Parts a–c of Figure 9 show the  $^1\text{H}$  PM-, DQ-, and SE-CRAMPS spectra of PAA2, respectively. The  $^1\text{H}$  DF-CRAMPS spectrum is not shown here, because no obvious signal of weakly coupled protons was observed for this vacuum-dried-sample. Compared with the  $^1\text{H}$  PM-CRAMPS spectrum shown in Figure 9a, the relative intensity of the peak at 12.9 ppm is greater than that of the peak at 10.7 ppm after DQ-filter shown in Figure 9b. Figure 9c shows the  $^1\text{H}$  SE-CRAMPS spectrum with proton transverse dephasing time  $\tau = 4$  ms, and two peaks at 12.9 and 10.7 ppm can be clearly identified. Since PAA2 is a vacuum-dried-sample with little residual water, predominate protons in this sample should be  $\text{H}_{\text{DM}}$  and  $\text{H}_{\text{FR}}$  besides the aliphatic protons. Therefore, the two strong peaks at 12.9 and 10.7 ppm in Figure 9b should be assigned to  $\text{H}_{\text{DM}}$  and  $\text{H}_{\text{FR}}$ , respectively. This assignment is consistent with the above results for PAA1. A small peak at about 8.7 ppm should be ascribed to the residual water signal. In addition, it is interesting to note that considerable intensity of  $\text{H}_{\text{FR}}$  signal at 10.7 ppm survives the DQ filter in Figures 8b and 9b. We suggest this could be predominately attributed to  $\text{H}_{\text{FR}}$  protons on the COOH group that forms an open dimer, this kind of non-hydrogen-bonded  $\text{H}_{\text{FR}}$  is strongly coupled with the  $\text{H}_{\text{DM}}$  proton of another COOH group (see Figure 2). As the result, there is considerable intensity of  $\text{H}_{\text{FR}}$

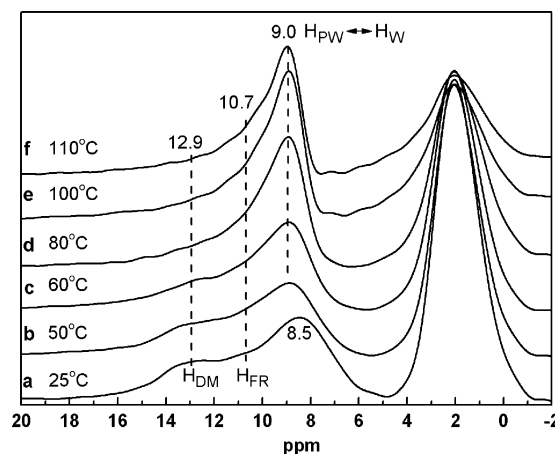


**Figure 10.** Temperature dependence of  $^1\text{H}$  PM-CRAMPS NMR spectra of PAA1 in the temperature range from 25 to 110  $^{\circ}\text{C}$ .

protons surviving the DQ filter. From the above experimental results, we can conclude that the dehydration of hydrated PAA promotes the formation of hydrogen bonds between COOH groups related to  $\text{H}_{\text{DM}}$ . The above NMR results also clearly indicate that the  $^1\text{H}$  DQ-, DF-, and SE-CRAMPS techniques are powerful tools to elucidate the structure and dynamics in solid polymers.

**3. Temperature Dependence of Various Hydrogen Bond Forms Determined by  $^1\text{H}$  VT-CRAMPS Experiments.** It is well-known that hydrogen bonding interaction is very sensitive to temperature. Detailed information about the formation and disassociation of hydrogen bonds with respect to temperature is crucial to the fundamental studies and applications for polymers and biopolymers. Dong et al.<sup>6a</sup> reported FT-IR and FT-Raman studies on the dissociation of hydrogen bonds at different temperatures in PAA, however, a good understanding of the temperature effect on the disassociation of these hydrogen bonds is still lacking. Since different types of hydrogen bonds can be direct discerned by the above  $^1\text{H}$  NMR methods, this allows us to direct determine the temperature dependence of various hydrogen bond forms in PAA by VT-CRAMPS experiment. On the other hand, by varying the temperature, the chemical exchange between protons of water and COOH groups can be further elucidated. It was reported that the formation of anhydride cross-links of the PAA samples is very slow and can be neglected below 150  $^{\circ}\text{C}$ .<sup>23</sup> Therefore, to prevent any changes of the chemical structure of the sample, all the VT-CRAMPS experiments were performed within the temperature range of 25–110  $^{\circ}\text{C}$  in the present work. Although  $^1\text{H}$  SE-CRAMPS experiment provides the best resolution than other  $^1\text{H}$  CRAMPS experiments, we still employed the  $^1\text{H}$  PM-CRAMPS technique in VT-CRAMPS experiments due to its high sensitivity.

Figure 10 shows the  $^1\text{H}$  PM-CRAMPS spectra of PAA1 as a function of temperature in the range from 25 to 110  $^{\circ}\text{C}$ . It is noteworthy that the intensity of the broad peak at 12.9 ppm ( $\text{H}_{\text{DM}}$ ) decreases with increasing temperature, and this peak is invisible when the temperature is higher than 60  $^{\circ}\text{C}$ , indicating a complete dissociation of  $\text{H}_{\text{DM}}$  related hydrogen bonds. To our knowledge, this the first direct NMR evidence of the dissociation of hydrogen bonds between COOH groups in hydrated PAA with increasing temperature. On the other hand, the water signal at 8.5 ppm decreases in relative intensity and shift to 9.0 ppm with increasing temperature from 25 to 50  $^{\circ}\text{C}$ , indicating a gradual departure of adsorbed water. With increasing temperature from 50 to 100  $^{\circ}\text{C}$ , the water signal is obviously narrowed and no hump in the range of 6–8 ppm can be found at 100  $^{\circ}\text{C}$

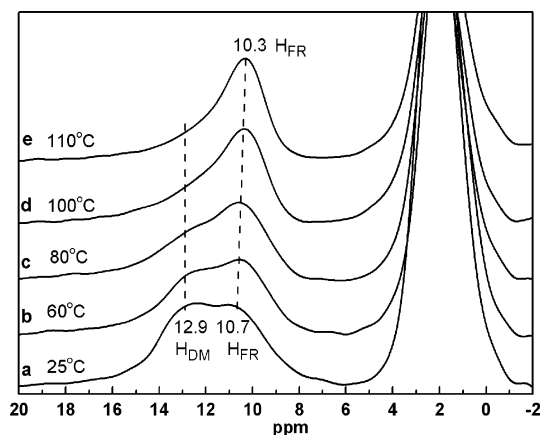


**Figure 11.** Temperature dependence of  $^1\text{H}$  PM-CRAMPS NMR spectra of PAA2 in the temperature range from 25 to 110  $^{\circ}\text{C}$ .

when compared with that at 25  $^{\circ}\text{C}$ . Meanwhile, the relative intensity of the water peak at 9 ppm obviously increases and this chemical shift keeps unchanged. This can be attributed to the enhancement of the fast chemical exchange between water and COOH protons (denoted as  $\text{H}_{\text{PW}} \leftrightarrow \text{H}_{\text{W}}$  in Figure 10) with increasing temperature. At a high temperature of 110  $^{\circ}\text{C}$ , the efficiency of DUMBO-1 dipolar decoupling decreases, resulting in the broadening and decreasing of all peaks. In addition, we can also observe a small hump (9–12 ppm) on the left side of the water peak (9 ppm) at high temperature; we suggest that this hump might be attributed to the  $\text{H}_{\text{FR}}$  signal partially arising from the disassociation of  $\text{H}_{\text{DM}}$  protons. It is very interesting to note that the dehydration of the bound water in hydrated PAA is not significant even at high temperature of 110  $^{\circ}\text{C}$ . In the following DSC and TGA experiments, the above conclusion can be further understood from the fact that no obvious dehydration can be observed even at the high temperature of 130  $^{\circ}\text{C}$  for the PAA1 samples.

Figure 11 shows the  $^1\text{H}$  PM-CRAMPS spectra of PAA2 as a function of temperature in the range from 25 to 110  $^{\circ}\text{C}$ . The intensity of  $\text{H}_{\text{DM}}$  at 12.9 ppm gradually decreases with increasing temperature. As mentioned earlier, this can be attributed to the dissociation of the hydrogen bonds between COOH groups. In contrast with the PAA1 sample, the dissociation of these hydrogen bonds in PAA2 occurs slowly over a wide range of temperature, and we can observe a small hump of the residual  $\text{H}_{\text{DM}}$  signal even at 110  $^{\circ}\text{C}$  as shown in Figure 11e. This indicates that the dissociation of the hydrogen bonds between COOH groups is easier for the PAA1 sample due to the existence of water. On the other hand, the relative intensity of the  $\text{H}_{\text{FR}}$  peak at 10.7 ppm gradually increases and shifts to 10.3 ppm with increasing temperature, which can be attributed to the increasing of  $\text{H}_{\text{FR}}$  signal partially arising from the disassociation of hydrogen bonds associated with  $\text{H}_{\text{DM}}$  protons with increasing temperature. It is very interesting to note that the chemical shifts of the retained peaks within 8–13 ppm for PAA1 and PAA2 at high temperature of 110  $^{\circ}\text{C}$  are quite different. The retained peak at 9.0 ppm of PAA1 (hydrated PAA) is attributed to  $\text{H}_{\text{PW}}$  and  $\text{H}_{\text{W}}$  protons undergoing fast chemical exchange, whereas the retained peak of PAA2 (dehydrated PAA) at 10.3 ppm should be attributed to the  $\text{H}_{\text{FR}}$  protons. This result implies that the dehydration of bound water in hydrated PAA should occur significantly at high temperature. The above VT-CRAMPS results are consistent with the foregoing assignment of different types of protons in PAA at room temperature.

It is also interesting to compare the present  $^1\text{H}$  VT-CRAMPS results with previous studies on the temperature dependence of

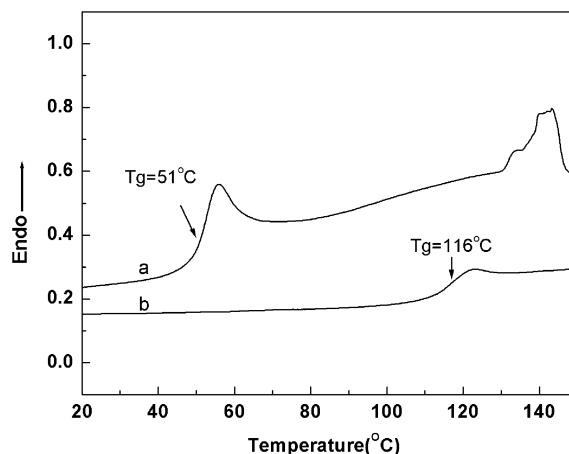


**Figure 12.** DSC traces of PAA1 in the (a) first and (b) second heating scan at a rate of 20  $^{\circ}\text{C}/\text{min}$ .

hydrogen bonds between COOH groups using other techniques. In previous work on PAA dried in vacuum condition using FT-IR and FT-Raman techniques over a temperature range of 40–140  $^{\circ}\text{C}$ ,<sup>6a</sup> different types of hydrogen-bond forms between COOH groups were suggested. It was found that different structures of hydrogen bond persist even when the temperature rises well above the glass transition temperature, and the COOH groups dissociate significantly at high temperatures. The above results are in good agreement with that of our VT-CRAMPS experiments for similarly dehydrated sample PAA2 used in our work. However, our NMR experiments indicate that only little hydrogen bonds between COOH groups can be observed at temperature (110  $^{\circ}\text{C}$ ) lower than the  $T_g$  (116  $^{\circ}\text{C}$ ) of PAA as shown in Figure 11e. For hydrated sample PAA1, our NMR experiments indicate that the dissociation of the hydrogen bonds between COOH groups occurs remarkably at lower temperature (60  $^{\circ}\text{C}$ ), and no obvious hydrogen bonds between COOH groups can be observed at a temperature of 110  $^{\circ}\text{C}$  as shown in Figure 10f.

**4. Comparison of  $^1\text{H}$  VT-CRAMPS and DSC Experimental Results for Hydrated PAA.** The DSC technique has been widely used to study the hydrogen bonding interaction in polymers, as well as different states of water in water-containing polymer and biopolymers.<sup>4b,c,23,24</sup> In order to get a better understanding of the temperature effect on the disassociation of different types of hydrogen bonds and to make a direct comparison between the present NMR results and that of DSC experiment, we further performed the DSC measurements for the PAA1 sample.

Figure 12 shows the DSC traces of the first and second heating scan of PAA1 containing 7 wt % water. For the first heating scan (Figure 12a), a glass transition was observed at 51  $^{\circ}\text{C}$  and a dramatic oscillating endothermic peak was observed at about 130  $^{\circ}\text{C}$ . For the second heating scan (Figure 12b), a clear glass transition at 116  $^{\circ}\text{C}$  was observed. Because of the departure of bounded water, the glass transition temperature in the second heating scan moves to 116  $^{\circ}\text{C}$  from 51  $^{\circ}\text{C}$ . It should be mentioned that the DSC trace of the second heating scan for PAA1 sample is equivalent to that for dehydrated sample PAA2. The lower glass transition temperature in the first heating scan compared with that in the second heating scan can be ascribed to the plasticizing effect of water. The above DSC results indicate that the glass transition temperature depends strongly on the water content. Figure 13 shows the TGA trace of the PAA1 sample at a heating rate of 20  $^{\circ}\text{C}/\text{min}$ . It is noticed that the dramatic oscillating endothermic peak observed after



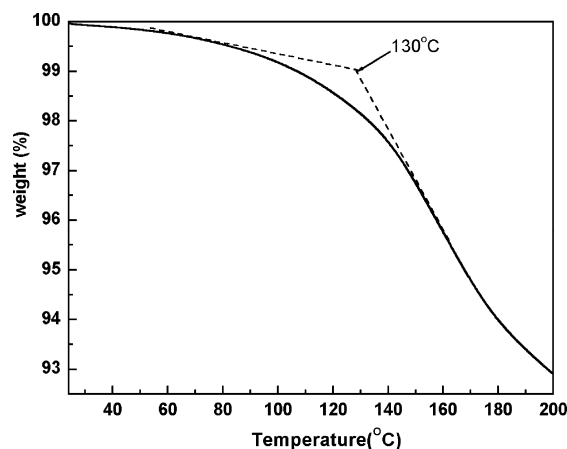


**Figure 13.** TGA trace of PAA1 at a heating rate of 20 °C/min.

130 °C in the first heating scan of DSC is well consistent with the beginning of the obvious losing of weight in the TGA trace. Therefore, it is reasonable to ascribe the dramatic oscillating endothermic peak in the first scan of DSC to the evaporation of the strong bound water. The above result is in good agreement with our VT-CRAMPS result shown in Figure 10f, which indicates that the departure of bound water in PAA1 is not significant even at high temperature of 110 °C. It is noteworthy that VT-CRAMPS NMR experiments in Figure 11 clearly reveal that the gradual dissociation of hydrogen bonds between COOH groups occurs with increasing temperature from 25 to 110 °C. However, in the DSC trace of the second heating scan for dehydrated PAA, nothing special could be observed before 100 °C through the featureless thermo trace. It should be mentioned that our present  $^1\text{H}$  CRAMPS NMR experiments cannot determine the glass transition of PAA1, since the observed disassociation of hydrogen bonds between COOH groups in Figure 10 is not directly associates with the glass transition of PAA1. Nevertheless, when compared with DSC experiments,  $^1\text{H}$  VT-CRAMPS experiments can provide detailed structural information about the temperature dependence of hydrogen bonds between COOH groups and water–polymer interaction in hydrated PAA at a molecular level.

**5. Water–Polymer Interaction and Proximity among Different Protons Determined by 2D  $^1\text{H}$ – $^1\text{H}$  Spin-Exchange Experiments.** Water–polymer interaction has crucial effect on the structure and properties of polymers. Although the interaction between water and polymer<sup>25</sup> or biological molecules<sup>16c,26</sup> has been extensively studied in recent years and well characterized by a variety of novel solid-state NMR techniques, little NMR work has been done on the water–polymer interaction for hydrated PAA. Recently, 2D  $^1\text{H}$ – $^1\text{H}$  spin-exchange spectra have been widely used to elucidate the  $^1\text{H}$ – $^1\text{H}$  proximity in organic solids and water–polymer interaction of biomacromolecules.<sup>8</sup> By using this technique, the water–polymer interaction and the proximity of different protons associated with different chemical groups in hydrated PAA can be elucidated.

Figure 14 shows 2D  $^1\text{H}$ – $^1\text{H}$  spin-exchange spectra of PAA1 in the chemical shift range of the COOH groups and water protons observed at room temperature with different mixing time. At the mixing time of 0.1 ms, no obvious exchange peak is observed as shown in Figure 14a. At the mixing time ( $\tau_{\text{sd}}$ ) of 0.5 ms, the most remarkable feature of the spectrum shown in Figure 14b can be found at the proton chemical shift range of 8–11 ppm, where we can clearly observe the cross-peak associated with water protons ( $\text{H}_\text{W}/\text{H}_\text{PW}$ ) at 8.5 ppm and free

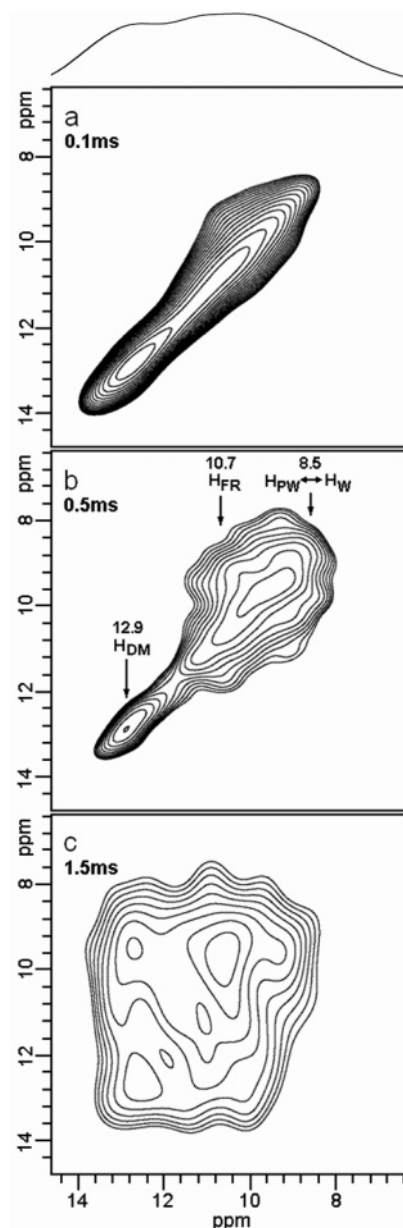


**Figure 14.** 2D  $^1\text{H}$ – $^1\text{H}$  spin-exchange NMR spectra of PAA1 acquired with mixing time ( $\tau_{\text{sd}}$ ) of (a) 0.1, (b) 0.5, and (c) 1.5 ms. A  $^1\text{H}$  projection is shown on top of the figure.

COOH groups ( $\text{H}_\text{FR}$ ) at 10.7 ppm. In principle, the cross-peak in  $^1\text{H}$ – $^1\text{H}$  spin-exchange spectrum can arise from either  $^1\text{H}$ – $^1\text{H}$  spin diffusion or from the chemical exchange. If chemical exchange occurs between  $\text{H}_\text{W}/\text{H}_\text{PW}$  and  $\text{H}_\text{FR}$  for 0.5 ms, the motion should lead a single peak (motional average). However, this was not observed in Figure 14b. Therefore, this cross-peak should arise from  $^1\text{H}$ – $^1\text{H}$  spin diffusion between  $\text{H}_\text{FR}$  and  $\text{H}_\text{W}/\text{H}_\text{PW}$  protons. Because spin diffusion depends on the dipolar coupling strength which is a function of the  $^1\text{H}$ – $^1\text{H}$  distance and local fluctuations (order parameters) that average it, and no cross-peak was found between  $\text{H}_\text{DM}$  and  $\text{H}_\text{W}/\text{H}_\text{PW}$  at mixing time of 0.5 ms, so it is reasonable to suggest that the adsorbed water is in proximity with free COOH groups ( $\text{H}_\text{FR}$ ) and far from the hydrogen bonds between COOH groups ( $\text{H}_\text{DM}$ ). At a very long mixing time, the spin-exchange should be spin-diffusion among all protons, thus cross-peaks between all protons should be observed. At the mixing time ( $\tau_{\text{sd}}$ ) of 1.5 ms (Figure 14c) we do observe the cross-peaks between all protons.

## Conclusion

We have carried a variety of continuous phase modulation multiple-pulse based high-resolution  $^1\text{H}$  CRAMPS NMR experiments to investigate various types of hydrogen bonds, their temperature dependence and water–polymer interaction in hydrated poly(acrylic acid). The  $^1\text{H}$  CRAMPS experiments revealed that there are four types of protons in hydrated PAA. These protons are assigned to protons from the mutually hydrogen-bonded COOH groups (1), from the free COOH groups (2), from the COOH groups bounded with water or from water bounded with COOH groups which are undergoing fast chemical exchange mutually (3), and from main chain groups (4), respectively. Furthermore, double-quantum filtered and dipolar filtered  $^1\text{H}$  CRAMPS experiments were proposed to further assign the protons according to their dipolar coupling strength. The high-resolution spin echo  $^1\text{H}$  CRAMPS experiments were further employed to accurately determine the chemical shift of these protons. These NMR techniques were also used to elucidate the molecular mobility of different group. It was found that the dehydration in PAA promotes the formation of hydrogen bonds between COOH groups. The variable-temperature  $^1\text{H}$  CRAMPS experiments demonstrated that the dissociation of the hydrogen bonds between COOH groups occurs dramatically at lower temperature in hydrated PAA and slowly over a wide range of temperature in dehydrated PAA. It was also found that the dehydration of water bounded with COOH groups in hydrated PAA occurs significantly at high temperature. These NMR results were compared with the DSC experimental results and that of previous work using other techniques. Besides undergoing fast chemical exchange, the adsorbed water was also demonstrated in proximity with the free COOH groups and far from the hydrogen bonds between COOH groups by using 2D  $^1\text{H}$ – $^1\text{H}$  spin-exchange NMR experiments. To the best of our knowledge, this is the first  $^1\text{H}$  SSNMR work using various continuous phase modulated CRAMPS techniques to detect different types of hydrogen bonds and their temperature dependence in solid polymer. We believe that the current systematic  $^1\text{H}$  SSNMR work provides a better understanding of the formation and disassociation of hydrogen bonds between COOH groups, as well as the water–polymer interaction in hydrated PAA. These  $^1\text{H}$  SSNMR methods can be expected to be further applied to the studies on a variety of PAA-containing polymers and provide useful structural and dynamic information at a molecular level for the development of advanced polymer materials based on poly(acrylic acid).

**Acknowledgment.** We are grateful to Dr. Siegfried Hafner for his helpful discussions on the CRAMPS techniques. This work was supported by National Natural Science Foundation of China (Grants 20374031, 50533020, 20474034, and 20634030), the Joint-Research Foundation of the Nankai and Tianjin Universities by the Chinese Ministry of Education, and the Program of New Century Excellent Talents in University. A.-C.S. acknowledges the support of the Natural Science and Engineering Council (NSERC) of Canada.

**Supporting Information Available:** Text giving the verification of  $^1\text{H}$  SSNMR experimental conditions for DUMBO-1 based  $^1\text{H}$  CRAMPS experiments and calibration of the scaling factor using alanine powder sample as a reference and figures showing the liquid-state  $^1\text{H}$  NMR spectra of PAA0 and PAA2. This material is available free of charge via the Internet at <http://pubs.acs.org>.

## References and Notes

- (1) (a) Tsuchida, E.; Abe, K. *Adv. Polym. Sci.* **1982**, *45*, 1. (b) Addad, C. J. P., Ed. *Physical Properties of Polymer Gels*; Wiley: Chichester, 1996. (c) He, Y.; Zhu, B.; Inoue, Y. *Prog. Polym. Sci.* **2004**, *29*, 1021. (d) Duffy, D. M.; Rodger, P. M. *J. Am. Chem. Soc.* **2002**, *124*, 5206. (e) Peng, C. C.; Abetz, V. *Macromolecules* **2005**, *38*, 5575.
- (2) (a) Perez, S. In *Water and Biological Macromolecules*; Westhof, E., Ed.; The Macmillan Press Ltd.: Houndmills, Basingstoke, London, 1993; Chapter 10, pp 295–320. (b) McBrierty, V. J.; Quinn, F. X.; Keely, C.; Wilson, A. C.; Friends, G. D. *Macromolecules* **1992**, *25*, 4281. (c) Heskins, M.; Guillet, J. E.; James, E. *Macromol. Sci. Chem.* **1968**, *A2*, 1441.
- (3) (a) Feindel, K. W.; Bergens, S. H.; Wasylishen, R. E. *ChemPhysChem* **2006**, *7*, 67. (b) Hietala, S.; Maunu, S. L.; Sundholm, F.; Lehtinen, T.; Sundholm, G. J. *Polym. Sci., Part B: Polym. Phys.* **1999**, *37*, 2893.
- (4) (a) Eisenberg, D.; Kauzman, W. *The Structure and Properties of Water*; Oxford University Press: London, 1969. (b) Takigami, S.; Kimura, T.; Nakamura, Y. *Polymer* **1993**, *34*, 604. (c) Higuchi, A.; Lijima, T. *Polymer* **1985**, *26*, 1207. (d) Sun, P. C.; Li, B. H.; Wang, Y. N.; Ma, J. B.; Ding, D. T.; He, B. L. *Eur. Polym. J.* **2003**, *39*, 1045. (e) Pontie, M.; Lemordant, D. *J. Membr. Sci.* **1998**, *141*, 13.
- (5) (a) Muroga, Y.; Noda, I.; Nagasawa, M. *Macromolecules* **1985**, *18*, 1576. (b) Quinn, J. F.; Caruso, F. *Langmuir* **2004**, *20*, 20. (PAA-LBL) (c) Lutkenhaus, J. L.; Hrabak, K. D.; McEnnis, K.; Hammond, P. T. *J. Am. Chem. Soc.* **2005**, *127*, 17228. (d) Khutoryanskiy, V. V.; Dubolazov, A. V.; Nurkeeva, Z. S.; Mun, G. A. *Langmuir* **2004**, *20*, 3785.
- (6) (a) Dong, J.; Ozaki, Y.; Nakashima, K. *Macromolecules* **1997**, *30*, 1111. (b) Tsukida, N.; Muranaka, H.; Ide, M.; Maeda, Y.; Kitano, H. *J. Phys. Chem. B* **1997**, *101*, 6676. (c) Tanaka, N.; Kitano, H.; Ise, N. *Macromolecules* **1991**, *24*, 3017. (d) Walczak, W. J.; Hoagland, D. A.; Hsu, S. L. *Macromolecules* **1992**, *25*, 7317. (e) Lu, X.; Weiss, R. A. *Macromolecules* **1995**, *28*, 3022.
- (7) (a) Schmidt-Rohr, K.; Spiess, H. W. *Multidimensional Solid-State NMR and Polymers*; Academic Press: San Diego, CA, 1994. (b) Tonelli, A. E. *NMR Spectroscopy and Polymer Microstructure*; VCH publisher: Weinheim, Germany, 1989.
- (8) (a) Brunner, E.; Sternberg, U. *Prog. Nucl. Magn. Reson. Spectrosc.* **1998**, *32*, 21. (b) Pawsey, S.; McCormick, M.; Paul, S. D.; Graf, R.; Lee, Y. S.; Reven, L.; Spiess, H. W. *J. Am. Chem. Soc.* **2003**, *125*, 4174. (c) Brus, J.; Dybal, J. *Macromolecules* **2002**, *35*, 10038. (d) Green, M. M.; White, J. L.; Mirau, P.; Scheinfeld, M. H. *Macromolecules* **2006**, *39*, 5971. (e) Brown, S. P.; Zhu, X. X.; Saalwachter, K.; Spiess, H. W. *J. Am. Chem. Soc.* **2001**, *123*, 4275. (f) Densmore, C. G.; Rasmussen, P. G.; Goward, G. R. *Macromolecules* **2005**, *38*, 416.
- (9) Garces, F. O.; Sivadason, K.; Somasundaran, P.; Turro, N. J. *Macromolecules* **1994**, *27*, 272.
- (10) (a) Miyoshi, T.; Takegoshi, K.; Terao, T. *Macromolecules* **1999**, *32*, 8914. (b) Miyoshi, T.; Takegoshi, K.; Hikichi, K. *Polymer* **1997**, *38*, 2315.
- (11) (a) Kinney, D. R.; Chuang, I. S.; Maciel, G. E. *J. Am. Chem. Soc.* **1996**, *118*, 5103. (b) Bronnimann, C. E.; Zeigler, R. C.; Maciel, G. E. *J. Am. Chem. Soc.* **1988**, *110*, 2023.
- (12) (a) Samoson, A.; Tuherm, T.; Gan, Z. *Solid State Nucl. Magn. Reson.* **2001**, *20*, 130.
- (13) (a) Gerstein, B. C.; Pembleton, R. G.; Wilson, R. C.; Ryan, L. M. *J. Chem. Phys.* **1977**, *66*, 361. (b) Burum, D. P.; Rhim, W. K. *J. Chem. Phys.* **1979**, *71*, 314.
- (14) (a) Sakellariou, D.; Lesage, A.; Hodgkinson, P.; Emsley, L. *Chem. Phys. Lett.* **2000**, *319*, 253. (b) Lesage, A.; Sakellariou, D.; Hediger, S.; Elena, B.; Charmont, P.; Steuarnagel, S.; Emsley, L. *J. Magn. Reson.* **2003**, *163*, 105. (c) Elena, B.; de Paepe, G.; Emsley, L. *Chem. Phys. Lett.* **2004**, *398*, 532. (d) Elena, B.; Emsley, L. *J. Am. Chem. Soc.* **2005**, *127*, 9140. (e) Lesage, A.; Duma, L.; Sakellariou, D.; Emsley, L. *J. Am. Chem. Soc.* **2001**, *123*, 5747.
- (15) (a) Hohwy, M.; Jakobsen, H. J.; Eden, M.; Levitt, M. H.; Nielsen, N. C. *J. Chem. Phys.* **1998**, *108*, 2686. (b) Madhu, P. K.; Vinogradov, E.; Vega, S. *Chem. Phys. Lett.* **2004**, *394*, 423. (c) Schnell, I. *Prog. Nucl. Magn. Reson.* **2004**, *45*, 145.
- (16) (a) Brown, S. P.; Lesage, A.; Elena, B.; Emsley, L. *J. Am. Chem. Soc.* **2004**, *126*, 13230. (b) Cherry, B. R.; Fujimoto, C. H.; Cornelius, C. J.; Alam, T. M. *Macromolecules* **2005**, *38*, 1201. (c) Lesage, A.; Emsley, L.; Penin, F.; Bockmann, A. *J. Am. Chem. Soc.* **2006**, *128*, 8246.
- (17) (a) Landfester, K.; Spiess, H. W. *Acta Polym.* **1998**, *49*, 451. (b) Egger, N.; Schmidt-Rohr, K.; Blumich, B.; Domke, W. D.; Stapp, B. *J. Appl. Polym. Sci.* **1992**, *44*, 289. (c) Mirau, P. A.; Yang, S. *Chem. Mater.* **2002**, *14*, 249. (d) Sun, P. C.; Dang, Q. Q.; Li, B. H.; Chen, T. H.; Wang, Y. N.; Lin, H.; Jin, Q. H.; Ding, D. T. *Macromolecules* **2005**, *38*, 5654.
- (18) Caravatti, P.; Neuenschwander, P.; Ernst, R. *Macromolecules* **1985**, *18*, 119.
- (19) (a) Xu, M.; Harris, K. D. M. *J. Am. Chem. Soc.* **2005**, *127*, 10832. (b) Nosaka, A. Y.; Watanabe, S.; Toyoda, I.; Nosaka, Y. *Macromolecules* **2006**, *39*, 4425. (c) Luo, W. B.; Hong, M. *Solid State Nucl. Magn. Reson.* **2006**, *29*, 163.

- (20) (a) Dvinskikh, S.; Castro, V.; Sandstrom, D. *Magn. Reson. Chem.* **2004**, *42*, 875. (b) Nicholls, A. W.; Mortishire-Smith, R. J. *Magn. Reson. Chem.* **2001**, *39*, 773. (c) Brus, J. *Solid State Nucl. Magn. Reson.* **2000**, *16*, 151.
- (21) (a) Meier, B. H.; Graf, F.; Ernst, R. R. *J. Chem. Phys.* **1982**, *76*, 767. (b) Berglund, B.; Vaughan, R. W. *J. Chem. Phys.* **1980**, *73*, 2037.
- (22) (a) Hafner, S.; Demco, D. E. *Solid State Nucl. Magn. Reson.* **2002**, *22*, 247. (b) Filip, C.; Hafner, S. *J. Magn. Reson.* **2000**, *147*, 250. (c) Hafner, S.; Spiess, H. W. *Concept. Magn. Reson.* **1998**, *10*, 99. (d) McDermott, A.; Ridenour, C.F. *The Encyclopedia of NMR*; Wiley: London, **1997**, 3820. (e) Liu, C. C.; Maciel, G. E. *Anal. Chem.* **1996**, *68*, 1401.
- (23) Maura, J. J.; Eustance, D. J.; Ratcliffe, C. T. *Macromolecules* **1987**, *20*, 196.
- (24) (a) Hatakeyama, T.; Quinn, F. X. *Thermal Analysis Fundamentals and Applications to Polymer Science*; New York: John Wiley & Sons, 1994; Chapter 2. (b) Froix, M. F.; Nelson, R. A. *Macromolecules* **1975**, *8*, 726.
- (25) (a) McCormick, M.; Smith, R. N.; Graf, R.; Barrett, C. J.; Reven, L.; Spiess, H. W. *Macromolecules* **2003**, *36*, 3616. (b) Ye, G.; Janzen, N.; Goward, G. R. *Macromolecules* **2006**, *39*, 3283.
- (26) (a) Lesage, A.; Bockmann, A. *J. Am. Chem. Soc.* **2003**, *125*, 13336. (b) Eliav, U.; Navon, G. *J. Am. Chem. Soc.* **2002**, *124*, 3125. (c) Otting, G. *Prog. Nucl. Magn. Reson. Spectrosc.* **1997**, *31*, 259.

MA070485C